

G/T Maximization of a Paraboloidal Reflector Fed by a Dipole-Disk Antenna with Ring by Using the Multiple-Reflection Approach and the Moment Method

Per-Simon Kildal, *Fellow, IEEE*, Svein A. Skyttemyr, and Ahmed A. Kishk, *Senior Member, IEEE*

Abstract—A 1.8-m paraboloidal reflector fed by a dipole-disk antenna with a beamforming ring is optimized for high G/T at L-band by using the moment method (MM) and the multiple reflection (MR) approach. The MR approach is based on using MM to calculate the radiation and scattering patterns of the feed, using physical optics plus uniform geometrical theory of diffraction (UTD) to include the reflector, and in addition to include the mutual interaction (multiple reflections) between the reflector and the feed by using the expression for the sum of an infinite geometric series. The MR approach is shown to be equally accurate as a MM solution of the complete antenna with reflector, provided the reflector is in the far field of the feed, and the MR approach is much faster. As a result of the calculations using the MR approach, design curves are presented showing how the G/T varies as a function of antenna geometry, size, and elevation angle, all for a given noise profile of the surrounding sky and ground. The computed radiation patterns and G/T s are compared with measurements for several elevation angles and surrounding terrain.

Index Terms— Reflector antennas.

I. INTRODUCTION

THE purpose of this paper is to describe the electrical design of a primary-fed reflector with 1.8-m diameter and a dipole feed at L-band for METEOSAT second generation. The design is optimized with respect to maximum G/T for low-elevation angles and linear polarization. The frequency band is 1691.0 ± 0.66 MHz.

The antenna selected for the study is that described in [1] and [2], a primary-fed paraboloidal reflector with a dipole-disk feed improved by a beamforming ring over the dipole (Fig. 1). The dipole is supported by an axial tube that contains the coaxial feed cables or itself represents a rigid coaxial feed line. Therefore, there is no need for support struts, and the antenna becomes completely rotationally symmetric (except for the dipole source). This is very advantageous from a computational point of view as the radiation pattern in this case is described completely in all ϕ planes by an analytic extension

Manuscript received October 24, 1995; revised August 22, 1996. This work was supported by ESTEC under contracts on the study of G/T of primary-fed reflectors at L-band for METEOSAT second-generation user stations.

P.-S. Kildal is with the Antenna Group, Chalmers University of Technology, Gothenburg, PS-41296 Sweden.

S. A. Skyttemyr is with Telenor Forskning, Kjeller, N-2007 Norway.

A. Kishk is with the University of Mississippi, University, MS 38677 USA.

Publisher Item Identifier S 0018-926X(97)04894-1.

from computed E - and H -plane patterns. Alternatively, such an analytic extension to all ϕ planes can be done from the co and cross-polar patterns in the 45° plane (see, e.g., [3]). This property simplifies the calculation of the antenna noise. The antenna is actually a typical BOR₁ antenna as defined in [4].

The purpose of the disk behind the dipole is to direct the dipole radiation toward the paraboloid. The beam forming ring equalizes the E - and H -plane patterns of the dipole and reduces the spillover loss as shown in [1] and [2].

The antenna picks up noise from the sky (including the atmosphere), the ground and from lossy components inside the antenna itself. Both the sky noise and the ground noise are functions of the elevation pointing angle of the antenna, the latter because the reflection coefficient of the ground is a function of angle of incidence. This means that a double integral covering all directions in space must be evaluated numerically in order to find the antenna noise temperature and this must be repeated for all elevation angles of the antenna. To simplify this, it is possible to solve the inner integral analytically by approximating the elevation dependence of the brightness temperature of the sky as shown in [6]. This makes the calculations both simpler and more efficient. Nevertheless, the computed results for the noise temperatures and G/T in the present paper are obtained only by using the exact formulas.

A computer program that calculates the G/T as a function of elevation pointing is developed. The inputs to the program are the co and cross-polar radiation patterns of the antenna in the 45° plane, as well as the ohmic losses in the feed line and the noise figure of the low-noise amplifier. The brightness temperature of the sky is included and is considered to be a function of elevation, as given in Table I. The tabulated values correspond approximately to those given in [5]. The table is extended to negative elevation angles, i.e., ground noise. The table represents for negative angles typical values of the temperature. In reality, the elevation variation will depend on the soil and roughness of the ground and on the polarization. The noise temperature calculations are based on [7, Sec. 8.6].

The radiation patterns are calculated by using:

- 1) the body of revolution program (AKBOR) of Kishk [8] based on the MM;
- 2) the latest multiple reflection (MR) version of the ELAB symmetrical antenna code (SAC MR) based on physical

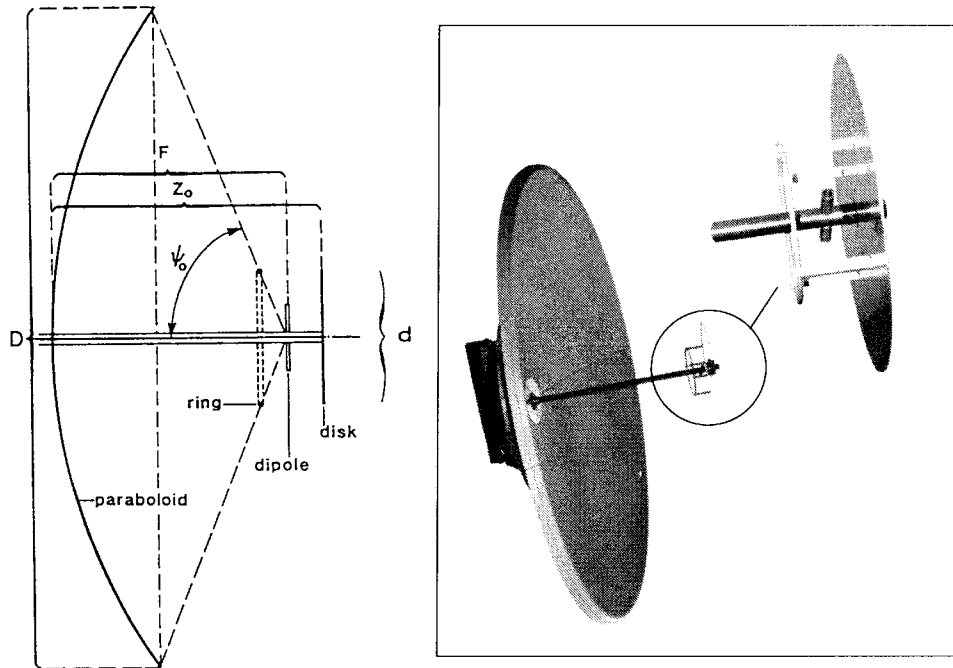


Fig. 1. Rotationally symmetric paraboloid with dipole-disk feed and beamforming ring.

TABLE I
TYPICAL BRIGHTNESS TEMPERATURE OF THE SKY AND GROUND
FOR $f = 2$ GHz AS A FUNCTION OF ELEVATION ANGLE [5]

Elevation	Temp	Elevation	Temp
90 deg	2.7 K	10 deg	14.7 K
80 deg	3.1 K	5 deg	29 K
70 deg	3.3 K	0 deg	80 K
60 deg	3.6 K	-5 deg	188 K
50 deg	3.84 K	-10 deg	260 K
40 deg	4.12 K	-15 deg	280 K
30 deg	4.4 K	-20 deg	288 K
20 deg	7.5 K	-25 deg	293 K
15 deg	10.2 K	-90 deg	293 K

optics (PO) integration for the near-in sidelobes and uniform geometrical theory of diffraction (UTD) for the far-out sidelobes, e.g., as described in [9]; this gives significantly shorter computer time than the AKBOR code—the old version of the SAC code is described in [10], and the MR version includes the MR between the feed and the reflector, as described in [11] and [12] (see also Section III).

Both computer programs can, in principle, be used to accurately calculate the radiation pattern of the total antenna including both the feed and the reflector, as all include in principle the mutual interaction (MR's) between the feed and the reflector. This effect is very important in reflector antennas that are only a few wavelengths in diameter, like most antennas at L-band. The antenna described in [2] has a 90-cm diameter and the gain was improved by 1 dB over standard predictions by controlling these MR's. The MR's can also, if not controlled, cause a gain reduction of more than 1 dB compared to standard predictions. For antennas with a 1.8-m diameter, the effect is normally smaller, but will be large for certain dimensions of the feed, so it still needs to be considered. Aperture blockage is automatically included by the MR approach (see Section III).

II. DESCRIPTION OF CALCULATION METHODS

We will consider antennas which have rotationally symmetric structures with respect to the z axis and are excited by halfwave dipoles oriented orthogonal to the z axis, chosen to point in the y direction. For such cases the radiation pattern of the antenna can be completely described in terms of its E - and H -plane patterns $E(\theta)$ and $H(\theta)$, respectively, according to (see [3])

$$\vec{E}(\theta, \varphi, r) = [E(\theta) \sin(\varphi) \hat{\theta} + H(\theta) \cos(\varphi) \hat{\varphi}] \frac{1}{r} e^{-jkr}. \quad (1)$$

(This description is exactly true only when the dipole is infinitely short, but represents a useful and good approximation also for halfwave dipoles, as explained in [4].) Note that $E(0) = H(0)$ always. Alternatively, the pattern can also be described by its co and cross-polar patterns in the 45° plane, $CO(\theta)$, and $XP(\theta)$, respectively, where (see also [3])

$$CO(\theta) = \frac{1}{2}[E(\theta) + H(\theta)], \quad XP(\theta) = \frac{1}{2}[E(\theta) - H(\theta)]. \quad (2)$$

Antennas that have radiation fields of the general forms in (1) and (2) are referred to in [4] as BOR₁ antennas due to the first-order sine/cosine variation with φ . These forms are also valid for the scattering patterns defined in [12]. The total power radiated by the antenna is (with the wave impedance suppressed and effective values used for the field quantities)

$$P_{\text{tot}} = \int \int_{4\pi} |\vec{E}(\theta, \varphi, r)|^2 r^2 d\Omega \\ = \pi \int_0^\pi [|E(\theta)|^2 + |H(\theta)|^2] \sin(\theta) d\theta. \quad (3)$$

The radiation pattern of the dipole-fed reflector can be calculated in several ways by using the SAC MR and AKBOR codes, three of which are described below.

- 1) The simplest way is to model the whole geometry, including feed and reflector, by using the MM (e.g., as implemented in the AKBOR program). We refer to this as the “MMtot approach.” The computer time will, in this case, be large. An advantage with MMtot is that even the axial support tube of the dipole feed can be included in the analysis.
- 2) The standard way would be to calculate the feed pattern by using MM and use this as input to the reflector antenna program for performing PO integration for the near-in sidelobes and UTD for the far-out sidelobes. We refer to this as the “PO/UTD approach.” This model may include the center blockage by using reflector-located blockage currents or more accurately by using obstacle-located blockage currents [13]. Both these blockage calculations are possible with the SAC MR code. However, the PO/UTD approach is, even with blockage included, not accurate since the mutual interactions between the feed and the reflector are not accounted for. In particular, the near-in sidelobes cannot be accurately predicted.
- 3) The third alternative is to use the multiple reflection approach built into the SAC MR code. Herein, we will refer to this approach as the “MR approach.” This approach makes use of the feed pattern as well as a scattering pattern of the feed, which both are easy and fast to calculate with MM using AKBOR. Note that the scattering pattern is herein calculated without the dipole present, as explained in [11]. These two patterns are used to form a new total feed pattern as described in Section III and, thereafter, PO and UTD are used as in the PO/UTD approach and the multiple reflections, as well as the center blockage effects, are automatically included via the total feed pattern without introducing any blockage currents in the PO analysis. The MR approach is described in [11], and a briefer description is given below. The MR approach has about the same computer time as the PO/UTD approach, but is much more accurate. However, it cannot include the axial support tube in the analysis as can the MMtot approach.

III. THE MULTIPLE REFLECTION APPROACH

The multiple reflection approach is based on the assumption that the aperture field of the paraboloid has constant phase over most of the aperture and constant amplitude over the central region that corresponds to the diameter of the primary feed. These approximations are valid if the primary feed has a small width in terms of wavelengths and is located with its phase center close to the focal point of the paraboloid.

To calculate the radiation pattern we need to know both the radiation pattern and the scattering pattern of the y -polarized feed in the feed coordinate system. This has its positive z axis pointing toward the center of the paraboloid. The radiation field of the feed when it is excited by the dipole current is of the form

$$\vec{E}_f(\theta, \varphi, r) = [E_f(\theta) \sin(\varphi) \hat{\theta} + H_f(\theta) \cos(\varphi) \hat{\varphi}] \frac{1}{r} e^{-jk r}. \quad (4)$$

where $E_f(\theta)$ and $H_f(\theta)$ are the E - and H -plane patterns, respectively. The scattering pattern is calculated by assuming an incident plane wave of unit amplitude and zero phase at $z = 0$ propagating in negative z -direction of the feed coordinate system, i.e.,

$$\vec{E}_p(x, y, z) = e^{jkz} \hat{y}. \quad (5)$$

The scattered E field of the feed due to this plane incident wave can be expressed as

$$\vec{E}_s(\theta, \varphi, r) = [E_s(\theta) \sin(\varphi) \hat{\theta} + H_s(\theta) \cos(\varphi) \hat{\varphi}] \frac{1}{r} e^{-jkr}. \quad (6)$$

where $E_s(\theta)$ and $H_s(\theta)$ are the E - and H -plane scattering patterns, respectively.

The phases of $E_f(\theta)$, $H_f(\theta)$, $E_s(\theta)$, and $H_s(\theta)$ are referred to $z = 0$ in the coordinate system of the feed. The phase center of the feed can be calculated by using the method in [14] and [15]. The phase reference points of $E_f(\theta)$, $H_f(\theta)$, $E_s(\theta)$, and $H_s(\theta)$ can be transformed to the phase center or to a point $z = z_0$ close to it by the following transformations:

$$\begin{aligned} E_f'(\theta) &= E_f(\theta) e^{-jkz_0 \cos \theta} \\ H_f'(\theta) &= H_f(\theta) e^{-jkz_0 \cos \theta} \\ E_s'(\theta) &= E_s(\theta) e^{-jkz_0(1+\cos \theta)} \\ H_s'(\theta) &= H_s(\theta) e^{-jkz_0(1+\cos \theta)}. \end{aligned} \quad (7)$$

The primed patterns are referred to $z = z_0$. These relations are easily derived by equating the E -fields calculated by (4) for unprimed and primed patterns at any observation point, where r in the unprimed case is the distance from the observation point to $z = 0$ and in the primed case the distance from the observation point to $z = z_0$. We see that the transformations are different for the feed pattern and the scattering pattern. This is because in the latter case both the plane wave excitation of the scattering pattern in (5) as well as the scattering pattern itself change, whereas in the former case the excitation of the feed pattern is the dipole current, which is independent of the coordinate system used.

We are now ready to formulate the MR approach. We assume that the reflector is paraboloidal and described by

$$r(\theta) = F / \cos^2(\theta/2) \quad (8)$$

in a reflector coordinate system located at the focal point and with z axis pointing toward the center of the reflector. We will, for simplicity, assume that the phase-reference point of the feed is at the focal point of the reflector, i.e., that the feed and reflector coordinate systems coincide. Therefore, if the feed is moved relative to the focal point, the phase reference point must be moved correspondingly.

Under these conditions, the incident field on its paraboloid due to the radiation pattern of the feed is

$$\vec{E}_i(\theta, \varphi) = [E_f(\theta) \sin(\varphi) \hat{\theta} + H_f(\theta) \cos(\varphi) \hat{\varphi}] \frac{1}{r(\theta)} e^{-jkr(\theta)}. \quad (9)$$

The aperture field at an axial location z becomes ($z = 0$ at the focal point)

$$\vec{E}_a(z) = -\vec{E}_i(\theta, \varphi) e^{-jk(-z+r(\theta) \cos \theta)} \quad (10)$$

where the minus sign is due to the reflection coefficient at the surface of the paraboloid. By using (8) we see that $r(\theta)(1 + \cos\theta) = 2F$ so that close to the z axis (where the copolar field dominates) we can write

$$\vec{E}_a(z) = -\text{CO}_f(0) \frac{1}{F} e^{-jk(2F-z)} \hat{y} \quad (11)$$

where $\text{CO}_f(0) = E_f(0) = H_f(0)$. This is local around the feed a plane wave. This plane wave aperture field will excite the feed and cause feed scattering. The scattered field becomes by using (6), (11), and the definition in (5)

$$\begin{aligned} \vec{E}_s(\theta, \varphi, r) &= (\vec{E}_a(0) \cdot \hat{y}) [E_s(\theta) \sin(\varphi) \hat{\theta} + H_s(\theta) \cos(\varphi) \hat{\phi}] \\ &\times \frac{1}{r} e^{-jkr}. \end{aligned} \quad (12)$$

The backward part of this scattered field will propagate toward the reflector, reflect, and cause another plane wave contribution to the aperture field. This will also scatter from the feed, propagate toward the reflector, reflect, and give rise to a third contribution to the aperture field. In fact, we will get an infinite sum of contributions to the aperture field of the form

$$\begin{aligned} \vec{E}_a(z) &= -\sum_{n=0}^{\infty} \text{CO}_f(0) \frac{1}{F} e^{-jk(2F-z)} \\ &\times \left[-\text{CO}_s(0) \frac{1}{F} e^{-j2kF} \right]^n \hat{y}. \end{aligned} \quad (13)$$

This is a geometric series and the sum becomes

$$\vec{E}_a(z) = \frac{-\hat{y} \text{CO}_f(0) \frac{1}{F} e^{-jk(2F-z)}}{[1 + \text{CO}_s(0) \frac{1}{F} e^{-j2kF}]}. \quad (14)$$

Thereby, the total field incident on the reflector can be written as the sum of (9) and (12) with $\vec{E}_a(0)$ given by (14). This total incident field represents a composite feed pattern.

When the incident field (i.e., composite feed pattern) has been found, the radiation field contribution of the reflector itself can be found by conventional PO integration over the reflector for the near-in sidelobes and UTD for the far-out sidelobes. This must be added to the direct radiation from the composite feed pattern, i.e., the sum of primary feed pattern (i.e., (9) with $r \rightarrow \infty$) and the scattering pattern of the feed (i.e., (12) with $r \rightarrow \infty$) to obtain the radiation pattern of the total antenna. It is important to note that the center blockage effect represents forward scattering from the feed when it is excited by the aperture field, so this is already built into the composite feed pattern and must not be included additionally in the PO integral. The scattering pattern has two major lobes, one in forward direction representing blockage and one in backward direction causing multiple reflections between the feed and the reflector.

The dipole impedance and, thereby, the total radiated power of the antenna is affected by the multiple reflections. Therefore, the total radiated power is herein found by integrating the radiation pattern of the total antenna using (3). The total radiated power is used to present the radiation patterns as directive gains in dBi.

IV. FORMULAS FOR ANTENNA NOISE

The radiation field of the total antenna (reflector plus feed) can also be expressed by (1) if we choose a coordinate system with a z axis along the main beam, i.e., opposite to the z axes of the feed and reflector coordinate system. The radiation power intensity as a function of θ and φ is (with the wave impedance suppressed)

$$\begin{aligned} p(\theta, \phi) &= |\vec{E}(r, \theta, \varphi)|^2 r^2 = p_E(\theta, \phi) + p_H(\theta, \phi) \\ p_E(\theta, \phi) &= |E(\theta)|^2 \sin^2 \phi; \quad p_H(\theta, \phi) = |H(\theta)|^2 \cos^2 \phi. \end{aligned} \quad (15)$$

We will now show how to calculate the antenna noise from $p_E(\theta, \phi)$ and $p_H(\theta, \phi)$. The brightness temperature $T_{\text{sky}}(\alpha)$ of the sky and the ground is a function of the elevation angle α , as discussed in Section II. The actual noise temperature seen by the antenna will be

$$T_{\text{ant}} = T_{E\text{ant}} + T_{H\text{ant}}$$

where

$$\begin{aligned} T_{E\text{ant}} &= \int_0^\pi \int_0^{2\pi} T_{\text{sky}}(\alpha) p_E(\theta, \varphi) \sin \theta d\phi d\theta / P_{\text{tot}} \\ T_{H\text{ant}} &= \int_0^\pi \int_0^{2\pi} T_{\text{sky}}(\alpha) p_H(\theta, \varphi) \sin \theta d\phi d\theta / P_{\text{tot}} \end{aligned} \quad (16)$$

with

$$\begin{aligned} P_{\text{tot}} &= \int_0^\pi \int_0^{2\pi} [p_E(\theta, \phi) + p_H(\theta, \phi)] \sin \theta d\phi d\theta \\ &= \pi \int_0^\pi [|E(\theta)|^2 + |H(\theta)|^2] \sin \theta d\theta. \end{aligned}$$

We will now express the elevation angle α in terms of the elevation pointing direction α_{el} of the main beam and θ and φ of the coordinate system of the antenna. We assume that the ground is an infinite plane. The polarization is either vertical or horizontal, the latter case is shown in Fig. 2. The coordinate system of the ground is $\hat{x}', \hat{y}', \hat{z}'$ and of the radiation pattern $\hat{x}, \hat{y}, \hat{z}$. A unit vector in r direction in the coordinate system of the antenna is described by $\hat{r} = \cos \theta \hat{z} + \sin \theta (\cos \phi \hat{x} + \sin \phi \hat{y})$. The angle θ' that \hat{r} makes with \hat{z}' is $\theta' = \arccos(\hat{r} \cdot \hat{z}')$. Thus,

$$\begin{aligned} \alpha &= (\pi/2) - \theta' = (\pi/2) \\ &\quad - \arccos(\cos \theta \sin \alpha_{\text{el}} - \sin \theta \cos \varphi \cos \alpha_{\text{el}}) \\ \alpha &= (\pi/2) - \theta' = (\pi/2) \\ &\quad - \arccos(\cos \theta \sin \alpha_{\text{el}} - \sin \theta \sin \varphi \cos \alpha_{\text{el}}) \end{aligned} \quad (17)$$

for horizontal and vertical polarizations, respectively.

Equation (16) can readily be integrated numerically. We have implemented them in the computer program for the G/T calculation. Testing shows that the φ integral is sufficiently accurately calculated if the φ range is divided in 32 intervals and the integrand is assumed constant over each; even 16 intervals work. The θ integral needs 180 intervals for 90-cm antennas and 360 intervals for 1.8-m and 4.0-m antennas at L-band. The same numbers are needed to obtain smooth plots of the radiation patterns.

The double integrals in (17) can be reduced to much more efficient single integrals if we assume that $T_{\text{sky}}(\alpha) =$

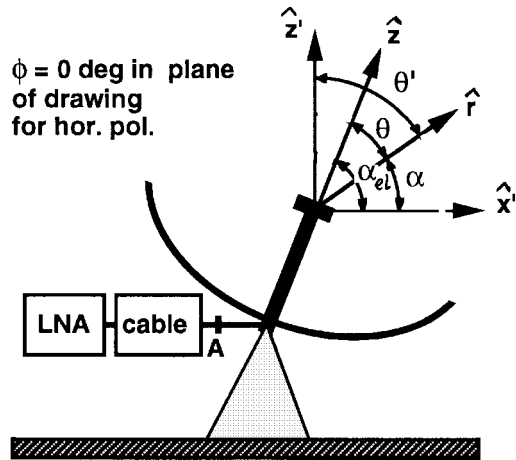


Fig. 2. Block diagram of receive antenna for noise calculation and coordinate system used to derive $\alpha = \alpha(\alpha_{el}, \theta, \varphi)$, illustrated for horizontal polarization.

$T_{sky}(\alpha_{el})$ for $\alpha > 0$ and $T_{sky}(\alpha) = T_0 = 293$ K for $\alpha < 0$. This is done in [6], but they are not used in the present paper.

V. CALCULATION OF G/T

We assume that the low-noise receiver (LNA) is connected to the antenna via a cable with losses. We even assume that all the ohmic loss, even in the feed and the reflectors, are included in the cable losses L_{dB} (in dB). The corresponding transmission efficiency is $\eta_c = 10^{-L_{dB}/10}$. The noise contribution from the cable loss is when referred to the antenna terminal A

$$T_c = T_0(1 - \eta_c)/\eta_c \quad (18)$$

with $T_0 = 293$ K the ambient temperature. The LNA has a noise factor NF_{dB} (in decibels). The corresponding noise temperature referred to the antenna terminal is

$$T_{rec} = 293 \text{ K} \cdot (10^{NF_{dB}/10} - 1)/\eta_c. \quad (19)$$

The antenna noise temperature T_{ant} is in the computer program calculated as explained in Section IV. $T_{sky}(\alpha_{el})$ is found by linear interpolation in Table I. Finally, the system noise temperature becomes

$$T_{sys} = T_c + T_{rec} + T_{ant}. \quad (20)$$

The gain of the antenna is $G = \eta_c G_0$ where G_0 is the directivity which is calculated by numerical integration of the total radiation pattern. Finally, the G/T becomes $G/T = G/T_{sys}$. We will also mention the aperture efficiency $\eta_a = G_0/(\pi D/\lambda)^2$ with D the reflector diameter.

VI. INITIAL MEASUREMENTS AND CALCULATIONS

Some initial measurements and calculations were done to verify the software. This was done with the feed dimension of [2] with and without the ring and located in a 1.8-m reflector. Several z locations of the feed were chosen to see if the methods could model the changes due to the multiple reflections. The first calculations were done by using AKBOR on the total antenna, i.e., by the MMtot approach. We tested the effect of the support tube and found it to be almost

negligible, so all calculations to follow are done without the support tube. We also tested how large effect the length of the dipole had on the results and found that the differences between infinitesimal and halfwave dipoles were negligible as well. Further, the MMtot approach was found to be able to predict the decreased sidelobes in H plane due to the ring. Also, when moving the feed 22 mm in and 22 mm out, so that the multiple reflection effect changes, AKBOR was able to predict the sidelobe changes. Calculations by using the MMtot and MR approaches were found to be nearly identical. The results obtained from the standard PO/UTD approach was not accurate. Center blockage was not included in the PO/UTD approach.

VII. OPTIMIZATION FOR HIGH G/T

A standard 1.8-m reflector with $F/D = 0.4$ was chosen of economical reasons. The remaining dimensions (i.e., feed location and size) were optimized to get as high G/T as possible for low-elevation angles. The dimensions that have the largest effect on the G/T was found to be the feed location and the diameter of the disk. Variations of the location of the ring and its diameter and thickness was tried but could not improve the results. Changes in the ring mainly caused higher cross-polar sidelobes and corresponding E - and H -plane unsymmetries. Such unsymmetries cannot be used to optimize the antenna as we need high G/T for both vertical and horizontal polarizations (even though the antenna has single linear polarization). The dipole length and height above the disk need to be close to half and quarter wavelengths, respectively, to get a good impedance match. Small variations around these values were found not to change the pattern and G/T significantly.

The reflector is deeper than required for maximum gain, so the ring around the dipole does not have much effect on the gain, but it improved the G/T considerably (see Table II). The reason was that the ring makes the feed pattern narrower in H plane. Therefore, we continued with optimizations with the ring.

The SAC MR program can easily be rerun several times with the same feed pattern and scattering pattern to provide results for different feed locations and reflector sizes. The reflector size is fixed in our case, but it is still of interest to calculate the aperture efficiency and the G/T as a function of reflector diameter to see whether the chosen reflector size corresponds to an interference maximum or minimum. Such results are presented in Figs. 3(a) and 4(a) for the case that the feed is located with the disk 0.2424λ behind the focal point of the paraboloid. Four different feeds with beamforming ring are studied, having different disk radii. For the smallest disk we see that the aperture efficiency has a small interference minimum when the reflector diameter has the given value of 10.3λ . However, when we increase the disk diameter to 2.2λ , there is an interference maximum for our reflector. We see the same typical behavior of the G/T for both 5° and 90° elevation angle. The latter case is shown in Fig. 4. For the 2.2λ disk diameter the multiple reflections are very strong and cause deep nulls in the efficiency and G/T curves for

TABLE II

DIMENSIONS, DIRECTIVITIES AND G/T 'S OF THE NONOPTIMUM 180-cm ANTENNA WHEN THE FEED IS WITHOUT (NORING) AND WITH (RING) RING AS WELL AS OF THE OPTIMUM ANTENNA (OPTIMUM). THE G/T 'S ARE GIVEN FOR HORIZONTAL POLARIZATION, BUT ARE ALMOST IDENTICAL FOR VERTICAL (LESS THAN 0.05-dB/K DIFFERENCE). THE DIRECTIVITIES AND G/T 'S ARE CALCULATED BY THE MMTOT APPROACH USING THE AKBOR PROGRAM. THE G/T RESULTS HAVE BEEN CALCULATED BY USING 0.1-dB OHMIC LOSSES AND 1.1-dB NOISE FIGURE OF THE RECEIVER

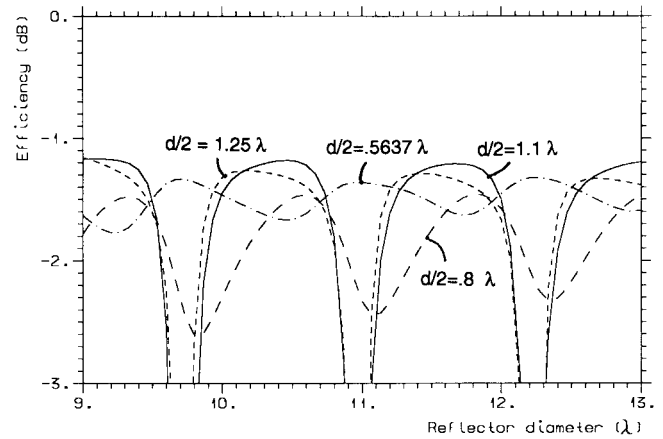
Case:	NORING	RING	Optimum
Wavelength	177 mm	177 mm	177 mm
Diameter of reflector	10.3151 λ	10.3151 λ	10.3151 λ
Disk/refl spacing $F - z_0$	4.3656 λ	4.3656 λ	4.3656 λ
Focal length F	4.1232 λ	4.1232 λ	4.1232 λ
Disk radius	0.5637 λ	0.5637 λ	1.1 λ
Ring location	no ring	0.4678 λ	0.4678 λ
Ring radius	no ring	0.5637 λ	0.5637 λ
Ring thickness (radius)	no ring	0.0169 λ	0.0169 λ
Calculated directivity	28.3 dBi	28.5 dBi	28.9 dBi
Calculated G/T at 5°	6.25 dB/K	6.92 dB/K	7.33 dB/K
Calculated G/T at 90°	7.01 dB/K	8.25 dB/K	8.59 dB/K

some reflector diameters. It is important to note that such variations of the G/T are a result of the multiple reflections and could not have been predicted with a standard PO/UTD approach.

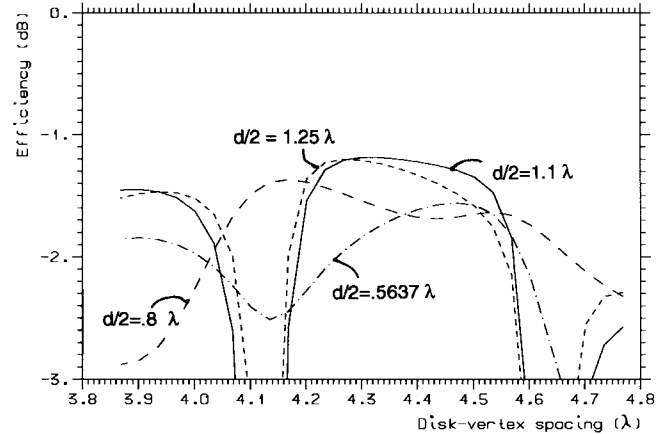
We have plotted similar curves as a function of the feed location in the given 1.8-m paraboloid in Figs. 3(b) and 4(b). The results are similar to Figs. 3(a) and 4(a). The 2.2λ disk is advantageous and has an interference maximum when the dipole is located in the focal point of the given paraboloid.

The optimum dimensions were chosen from Figs. 3 and 4. They are summarized in Table II and compared with the nonoptimum cases without and with beamforming ring. The calculated and measured radiation patterns for the optimum antenna are presented in Fig. 5. The discrepancy in the low sidelobe regions are due to the measured accuracy. We do not know the reason for the discrepancies of the first sidelobe in E plane. It may be due to the axial feed-support tube or the plastic supports of the beamforming ring. The radiation patterns calculated by the MMTot approach and the MR approach are compared in Fig. 6. The agreement is very good.

In Fig. 7, we have compared the optimum antenna with an antenna having exactly the same feed and F/D ratio, but with a reflector diameter of 11.0λ instead of 10.3λ . This diameter corresponds to an interference minimum in the efficiency curve in Fig. 3(a) and we clearly see that this antenna is nonoptimum. It has 2-dB lower directivity (even though the diameter is larger) and much higher sidelobes. This difference is entirely an effect of the multiple reflections. It should be mentioned that, for this interference minimum, the agreement between the MR and MMTot approaches is not so good. Investigations showed that the MR approach predicts too low gain in the interference minima, mainly due to an erroneous shape of the main lobe. The sidelobes agree better. Therefore, the curves in Figs. 3 and 4 (which are calculated by the MR approach) are not accurate in their minima. The minima seems to be shallower when calculated with the more correct MMTot approach.



(a)



(b)

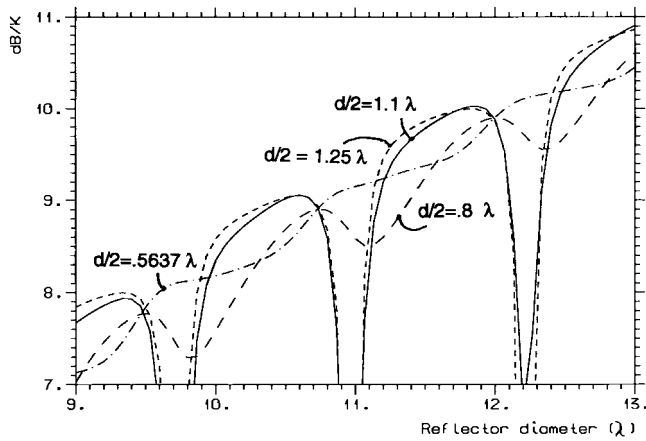
Fig. 3. Aperture efficiency of paraboloid with dipole-disk feed with beamforming ring for different diameters d of the disk computed by MR approach using AKBOR and SAC MR. The F/D ratio of the paraboloid is 0.4. (a) As a function of the reflector diameter when the dipole is located in focus. (b) As a function of the spacing between the disk and the vertex of the paraboloid for a reflector diameter of $D = 10.3151\lambda$.

VIII. RELATIVE G/T RESULTS

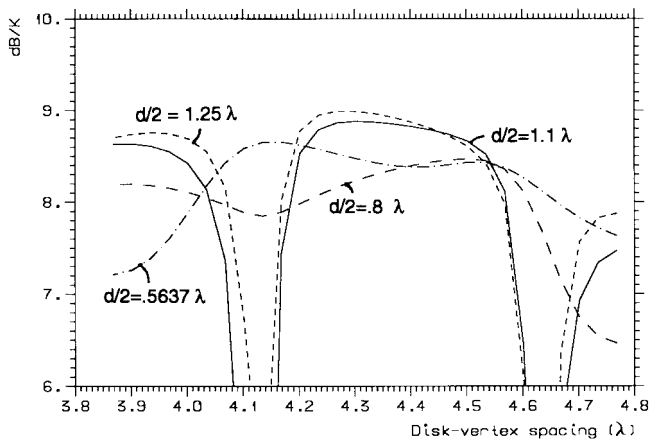
Fig. 8 presents G/T as a function of elevation for four different antennas with significantly different G/T . The four antennas are the optimized antenna in the previous section (OPTIMUM) and the RING and NORING cases in Table II. In addition, we have included the G/T of the NORING case with 0.4 dB losses in the feed instead of 0.1 dB. Fig. 8(a) shows a significant difference in G/T of the four cases. The G/T improves by 0.6 to 0.9 dB by reducing the losses in the feed line from 0.4 to 0.1 dB, it improves by another 0.6–1.25 dB by including the ring and it improves by another 0.3–0.6 dB by increasing the disk diameter to benefit from increased multiple reflections. We also see that the optimum antenna is clearly best at all elevation angles.

IX. EXPERIMENTS

We built two different dipole-disk feeds and measured the radiation patterns, gains, and G/T 's of each of them when mounted in a 1.8-m reflector antenna with $F/D = 0.4$. The feeds are called OPTIMUM and NORING, respectively,



(a)

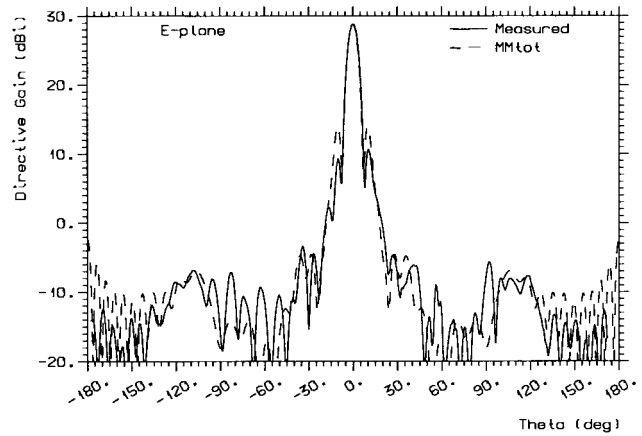


(b)

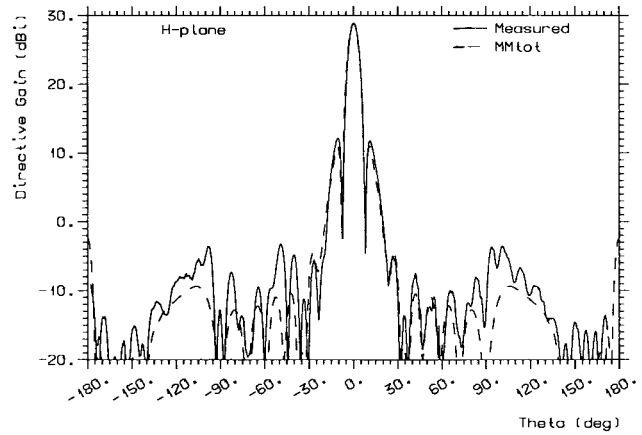
Fig. 4. G/T of paraboloid with dipole-disk feed with beamforming ring for different diameters d of the disk, computed by MR approach using AKBOR and SAC MR. The F/D ratio of the paraboloid is 0.4. The elevation angle is 90° , there are 0.1-dB ohmic losses, and the noise figure of the receiver is 1.1 dB. (a) As a function of the reflector diameter when the dipole is located in focus. (b) As a function of the spacing between the disk and the vertex of the paraboloid for a reflector diameter of $D = 10.3151\lambda$.

(see Table II). The optimum feed has a large disk and a beamforming ring, and the NORING feed has a small disk and is without ring. Otherwise, the feeds are identical, having a dipole fed through a coaxial line made of two coaxial metal tubes, thereby, no lossy cable is needed. The outer tube is also the support for the feed. We have a shielded slot-type balun between the coaxial line and the dipole. The balun consists of two half-wavelength longitudinal slots. The two monopoles that make up the dipole are connected to the outer-conductor orthogonal to the slots halfway between the slot ends. One of the monopoles has a connection to the inner conductor at the same point. To avoid undesired radiation from the balun, the slots are shielded by a third tube. Therefore, at the balun, the coaxial line has a smaller diameter (still with $50\text{-}\Omega$ impedance), while the outer tube change from being the outer conductor to a shield. The two monopoles are mounted to the outer conductor via two holes in the shield. Photos of the optimum feed and the 1.8-m L-band antenna are shown in Fig. 1.

The complex feed structure makes the antenna difficult to impedance match. As the multiple reflections are important,



(a)

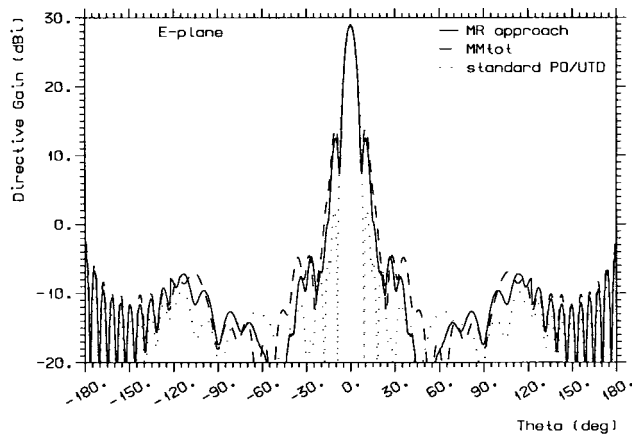


(b)

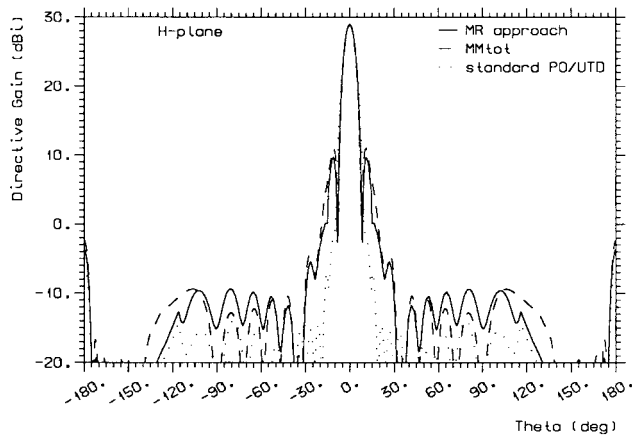
Fig. 5. Measured and computed radiation patterns of optimized 1.8-m reflector with dipole-disk feed (OPTIMUM case). (a) E plane. (b) H plane.

we cannot impedance match the feed in free space. The whole antenna system must be matched as one unit. To obtain a good impedance match, we used a rather thick dipole (15-mm diameter). With this dipole we got a very large return loss (36.7 dB) at 1690 MHz for the optimum antenna. The bandwidth with $\text{VSWR} < 1.5$ was 60 MHz. For the NORING antenna, the return loss was smaller (20.9 dB), but it had a wider bandwidth (100 MHz for $\text{VSWR} < 1.5$).

The gain for the optimum antenna was measured to be 28.5 dBi and for the NORING antenna 27.7 dBi. This is 0.3 and 0.5 dB lower than the theoretical values (Table II with 0.1-dB loss). The measurement accuracy was not better than 0.5 dB. We also calculated the directivity from the measured radiation patterns and obtained 28.9 dBi for the optimum antenna and 28.1 dBi for the NORING antenna. These values are respectively equal to and 0.2 dB lower than the directivities calculated by the AKBOR program. We found the G/T for the 1.8-m antenna at L-band by measuring the carrier-to-noise ratio C/N and using $G/T_{\text{dB}} = C/N_{\text{dB}} - \text{EIRP}_{\text{dB}} + L_{\text{dB}} + k_{\text{dB}} + B_{\text{dB}}$ where EIRP_{dB} is the equivalent isotropic radiated power in dB, L_{dB} is the space attenuation in dB, k_{dB} is Boltzmann's constant in dB and B_{dB} is the noise bandwidth in dB. The receiver chain had a measured noise factor of 1.0 dB and we used horizontal polarization. We measured C/N



(a)



(b)

Fig. 6. Radiation patterns of optimized 1.8-m reflector with dipole-disk feed (OPTIMUM case) calculated by the MMtot and MR approaches as well as by the standard PO/UTD approach. (a) E plane. (b) H plane.

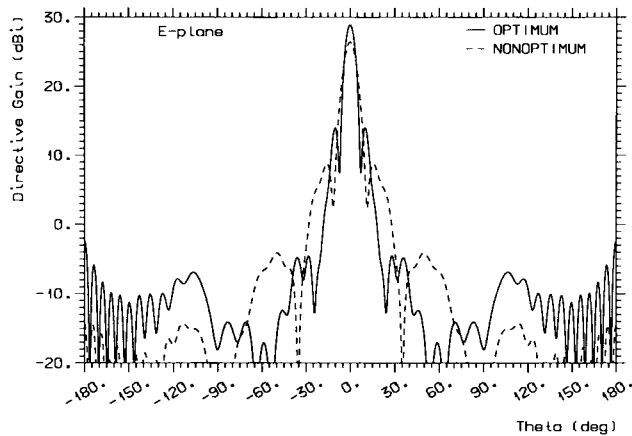
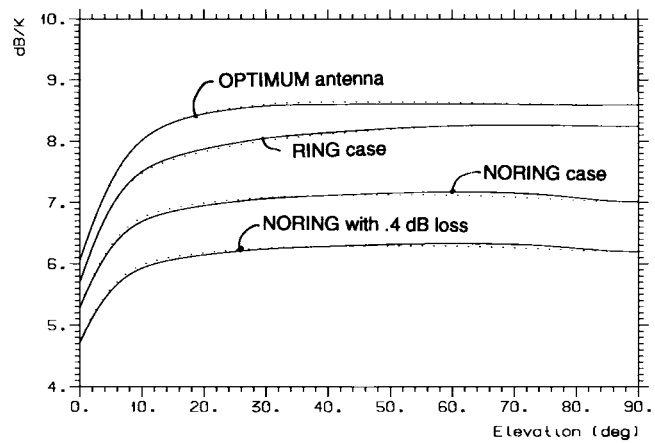
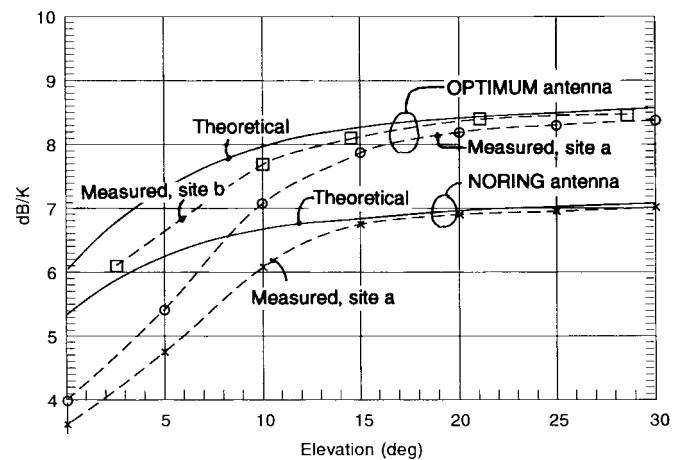


Fig. 7. E -plane patterns of the OPTIMUM antenna and a NONOPTIMUM antenna which has exactly the same feed as the OPTIMUM case and a reflector with the same F/D , but the reflector diameter is 11.0λ instead of 10.31λ as for the OPTIMUM case.

at zero elevation angle with the transmitter and the antenna placed on the roofs of two different buildings. The noise level was then measured while tilting the antennas to obtain higher elevation angles. G/T was calculated from the measurements as a function of elevation angle for two different sites, the roof



(a)



(b)

Fig. 8. (a) G/T as a function of elevation for different antenna solutions computed by MMtot approach using the AKBOR code. The solid lines represent horizontal polarization and the dotted lines vertical polarization. The receiver noise factor is 1.1 dB. The ohmic losses are 0.1 dB except for the lowest NORING curves. (b) Measured and calculated G/T . The calculated values are shown with solid lines, for the OPTIMUM antenna (upper curve) and the NORING antenna (lower curve). The measured values for the optimum antenna at sites a and b are shown as dashed lines.

of a building in a low area with several surrounding buildings (site a) and at the top of a hill with low hills and flat fields in front (site b). The results are compared with calculated values in Fig. 8. At low elevation angles we measure G/T values that are 2-dB lower than the calculations for site a , whereas they are about 0.5-dB lower for site b . This is reasonable, as site b is closer to the site of the theoretical noise profile, i.e., an ideal case with a flat ground, no unwanted reflections and no manmade noise. At higher elevation angles ($>15^\circ$) we avoid (more or less) these unwanted contributions to the noise and the measured values approach the theoretical ones closely.

X. OTHER REFLECTOR DIAMETERS

When planning a microwave system it is important to know how the G/T varies with the reflector diameter for the given frequency. Therefore, we have included Figs. 9 and 10. The results are presented for reflectors with $F/D = 0.4$ as above.

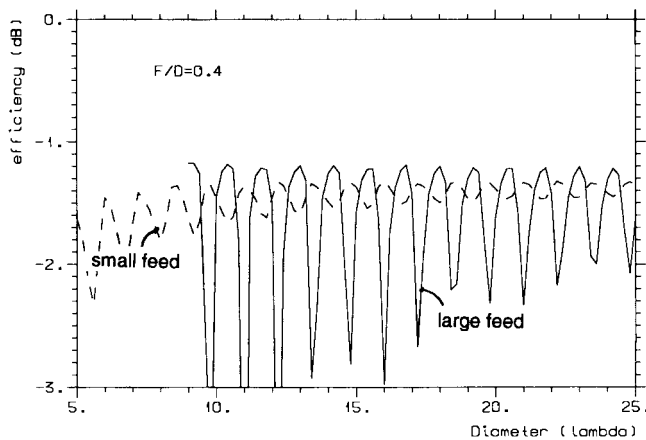


Fig. 9. Aperture efficiencies as a function of reflector diameter for paraboloidal reflectors with dipole disk feed and beamforming ring, for two different sets of feed dimensions and $F/D = 0.4$. The small feed has a disk radius of 0.5637λ and the large has 1.1λ . The remaining feed dimensions are equal and the same as the RING and OPTIMUM cases in Table II.

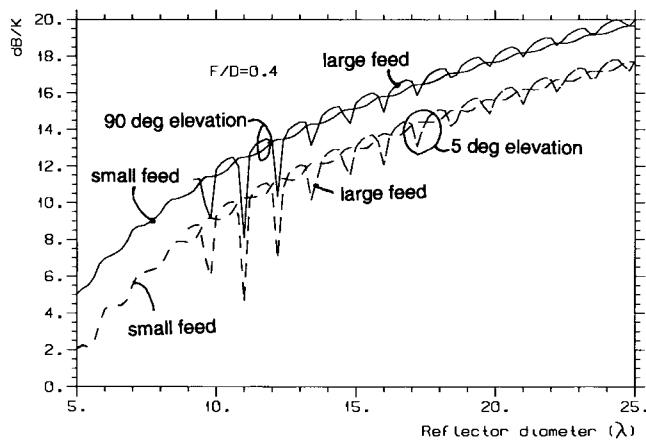


Fig. 10. Best G/T as a function of reflector diameter for reflectors with $F/D = 0.4$ fed by dipole disk feed with beamforming ring, for two different sets of feed dimensions. The small and large feeds have the same dimensions as in Fig. 9. The upper two curves are for 90° elevation angle and the lower two for 5° .

More results for deeper reflectors with $F/D = 0.33$ are given in [6].

The results are shown for two different feed dimensions, referred to as the small and large feed, corresponding to the feed dimensions in Table II for the RING and OPTIMUM cases, respectively. The small feed is optimum in the reflectors with small diameters, and the large feed is optimum in large reflectors. The curves for the large feeds are truncated for reflector diameters smaller than nine wavelengths because the MR approach then becomes inaccurate (the reflector comes in the near field of the feed). The frequency is the same as before and the polarization is horizontal. The noise figure of the LNA is now taken to be 0.4 dB which is also commercially available. The ohmic losses in the feed is assumed to be 0.1 dB. The noise profile in Table I is used. In reality, this noise will depend on the surroundings of the antenna, in particular for elevation angles below 20° .

The periodic peaks and dips in the efficiency and G/T curves are present over the whole range of reflector diameters.

Please note the following: if a reflector with a given diameter gives a G/T , which is low due to a dip on the curve, the location of the feed can always be tuned (i.e., defocused a little) to obtain the same G/T as at the closest G/T peak on the left side of the low value. Therefore, the peaks of the curves represent the best G/T values for all diameters, even those corresponding to minima in the curves. We also see that the peaks of the curves for small feeds occur between the peaks of the large feeds.

The results in [6] show that both the aperture efficiencies and the G/T 's of the deep ($F/D = 0.33$) reflectors are lower than the more shallow ($F/D = 0.4$) reflectors. This means that a deep reflector must have one to two wavelengths larger diameter to give the same G/T as a shallow reflector when the feed is a dipole-disk feed with beamforming ring.

XI. CONCLUSION

A 1.8-m reflector with a dipole-disk feed with ring has been optimized for high G/T at L-band for low elevation. The optimization has been done by calculating the pattern using the MR approach and integrating the pattern to obtain the G/T . The results have been checked by using MM on the total antenna and by measurements. The MR approach was found to be very accurate for the studied case and made it possible to present design curves which otherwise would have taken very long time to produce. Actually, no one of the curves in Figs. 3 and 4 and even Figs. 9 and 10 takes more than a few minutes to calculate.

The following conclusions are a result of the study: the G/T is almost identical for horizontal and vertical polarization. The beamforming ring of the feed gives a major improvement of the G/T . The G/T can in addition be considerably improved by increasing the disk diameter and controlling the multiple reflections to obtain resonance. The resulting optimum antenna can be called a resonant reflector antenna, as introduced in [2]. The noise figure of the receiver has a major effect on the G/T . Low-noise amplifiers with noise figures as low as $NF = 0.4$ dB are commercially available. The ohmic losses must be kept to a minimum; 0.3-dB loss decrease the G/T with 0.8 dB. The optimized antenna is optimum for low (5°) and nearly optimum for high (90°) elevation angles. If the multiple reflections are not controlled properly, they may cause large gain reductions of several decibels. The G/T varies with the surrounding terrain in particular for low-elevation angles.

It should also be noted that the elevation dependence of the brightness temperature of the sky that has been used is typical (see Table I). In reality, it will depend on the ground conditions and the polarization for low-elevation angles.

Finally, it should be mentioned that the quality of an antenna for low-elevation angles also will be determined by its ability to reduce multipath fading due to, e.g., ground reflections. Multipath is reduced if the sidelobes are low (multipath has not been treated in the present paper).

ACKNOWLEDGMENT

The authors would like to thank C. Markland and K. van t'Klooster at ESTEC, Noordwijk, The Netherlands, for their

comments and corrections to the work. We are also grateful to M. Viberg for detecting an important typographical sign error in one of the equations.

REFERENCES

- [1] P.-S. Kildal and S. A. Skyttemyr, "Dipole-disk antenna with beamforming ring," *IEEE Trans. Antennas Propagat.*, vol. AP-30, pp. 529–534, July 1982.
- [2] P.-S. Kildal, "A small dipole-fed resonant reflector antenna with high efficiency, low cross polarization and low sidelobes," *IEEE Trans. Antennas Propagat.*, vol. AP-33, pp. 1386–1391, Dec. 1985.
- [3] ———, "Factorization of the feed efficiency of paraboloids and Cassegrain antennas," *IEEE Trans. Antennas Propagat.*, vol. AP-33, pp. 903–908, Aug. 1985.
- [4] P.-S. Kildal and Z. Sipus, "Classification of rotationally symmetric antennas in BOR₀ and BOR₁ types," *IEEE Antennas Propagat. Mag.*, vol. 37, pp. 114–117, Dec. 1995.
- [5] Rep. CCIR, 1990; Rep. 720-2, Fig. 5, 1990.
- [6] P.-S. Kildal, S. Skyttemyr, and A. A. Kishk, " G/T maximization of a paraboloidal reflector fed by a dipole-disk antenna with ring by using the multiple-reflection approach and the moment method," in *Manufacture and Test of an Antenna and Measurement of Faraday Rotation*, ESTEC/Contract no. 11041/94/NL/CN, Dec. 1995, vol. 1, pt. 1, TeleNor FoU-Rep.
- [7] M. I. Skolnik, *Introduction to Radar Systems*. Tokyo, Japan: McGraw-Hill, Kogakusha, Ltd., 1962.
- [8] A. Kishk, "Electromagnetic scattering from composite objects using a mixture of exact and impedance boundary conditions," *IEEE Trans. Antennas Propagat.*, vol. 39, pp. 826–833, June 1991.
- [9] W. V. T. Rusch, "Reflector antennas," in *Numerical and Asymptotic Techniques in Electromagnetics*, R. Mittra, Ed. Berlin: Springer-Verlag, 1975, ch. 7.
- [10] P.-S. Kildal, E. Lier, and E. Olsen, "Efficient computer programs for study and optimization of blockage and diffraction in symmetrical reflector antennas," in *Proc. IEEE-APS/URSI Symp.*, Philadelphia, PA, June 1986, vol. I, pp. 469–472.
- [11] A. Moldsvor and P.-S. Kildal, "Feed scattering in primary-fed reflector antennas," in *Eur. Microwave Conf.*, Stockholm, Sweden, Sept. 1988, pp. 488–493.
- [12] ———, "A systematic approach to control feed scattering and multiple reflections in symmetrical primary-fed reflector antennas," *Proc. Inst. Elect. Eng.*, vol. 139, pt. H, no. 1, pp. 65–71, Feb. 1992.
- [13] ———, "Analysis of aperture blockage in reflector antennas by using obstacle-located blockage currents," *IEEE Trans. Antennas Propagat.*, vol. 40, pp. 100–102, Jan. 1992.
- [14] P.-S. Kildal, "Combined E - and H -plane phase-centers of antenna feeds," *IEEE Trans. Antennas Propagat.*, vol. AP-31, pp. 199–202, Jan. 1983.
- [15] ———, "Comments on 'Phase center calculation of reflector antenna feeds'" (by K. S. Rao and L. Shafai), *IEEE Trans. Antennas Propagat.*, vol. AP-33, pp. 579–580, May 1985.
- [16] ———, "Dipole feed," Norwegian Patent 148579.

Per-Simon Kildal (M'82–SM'84–F'95), for photograph and biography, see p. 1192 of the August 1996 issue of this TRANSACTIONS.



Svein A. Skyttemyr was born in Norway on April 27, 1956. He received the M.S.E.E. degree from the University of Trondheim, The Norwegian Institute of Technology (NTH), Trondheim, Norway, in 1979.

From 1980 to 1981, he was at ELAB (The Electronics Research Laboratory at NTH). Since 1981 he has been at Telenor Research and Development (formerly Norwegian Telecom Research), Kjeller, Norway. He is currently working with antennas and satellite communication systems.

Ahmed A. Kishk (S'84–M'86–SM'90), for photograph and biography, see p. 1519 of the November 1996 issue of this TRANSACTIONS.